The role of fission on neutron star mergers and its impact on the r-process peaks

M. Eichler' , A. Arcones, A. Kelic, O. Korobkin, K. Langanke, T. Marketin, G. Martinez-Pinedo, I. Panov, T. Rauscher, S. Rosswog, C. Winteler, N. T. Zinner, and F.-K. Thielemann

Citation: AIP Conference Proceedings **1743**, 040004 (2016); doi: 10.1063/1.4953296

View online: http://dx.doi.org/10.1063/1.4953296

View Table of Contents: http://aip.scitation.org/toc/apc/1743/1

Published by the American Institute of Physics

The Role of Fission on Neutron Star Mergers and its Impact on the r-Process Peaks

M. Eichler[1,a)], A. Arcones[2,3], A. Kelic[3], O. Korobkin[4], K. Langanke[2,3], T. Marketin[5], G. Martinez-Pinedo[2,3], I. Panov[6,1], T. Rauscher[7,1], S. Rosswog[4], C. Winteler[8], N. T. Zinner[9] and F.-K. Thielemann[1]

[1]*Department of Physics, University of Basel, Klingelbergstrasse 82, CH-4055 Basel, Switzerland*
[2]*Institut für Kernphysik, Technische Universität Darmstadt, Schlossgartenstrasse 2, D-64289 Darmstadt, Germany*
[3]*GSI Helmholtzzentrum fr Schwerionenforschung GmbH, Planckstrasse 1, D-64291 Darmstadt, Germany*
[4]*The Oskar Klein Centre, Department of Astronomy, AlbaNova, Stockholm University, SE-10691 Stockholm, Sweden*
[5]*Department of Physics, Faculty of Science, University of Zagreb, 10000 Zagreb, Croatia*
[6]*SSC RF ITEP of NRC "Kurchatov Institute", Bolshaya Cheremushkinskaya 25, 117218 Moscow, Russia*
[7]*Centre for Astrophysics Research, School of Physics, Astronomy and Mathematics, University of Hertfordshire, Hatfield AL10 9AB, UK*
[8]*Institut Energie am Bau, Fachhochschule Nordwestschweiz, St. Jakobs-Strasse 84, 4132 Muttenz, Switzerland*
[9]*Department of Physics and Astronomy, Aarhus University, Ny Munkegade, bygn. 1520, DK-8000 Aarhus C, Denmark*

[a)]Corresponding author: marius.eichler@unibas.ch

Abstract. The comparison between observational abundance features and those obtained from nucleosynthesis predictions of stellar evolution and/or explosion simulations can scrutinize two aspects: (a) the conditions in the astrophysical production site and (b) the quality of the nuclear physics input utilized. Here we test the abundance features of r-process nucleosynthesis calculations using four different fission fragment distribution models. Furthermore, we explore the origin of a shift in the third r-process peak position in comparison with the solar r-process abundances which has been noticed in a number of merger nucleosynthesis predictions. We show that this shift occurs during the r-process freeze-out when neutron captures and β-decays compete and an (n,γ)-(γ,n) equilibrium is not maintained anymore. During this phase neutrons originate mainly from fission of material above $A = 240$. We also investigate the role of β-decay half-lives from recent theoretical advances, which lead either to a smaller amount of fissioning nuclei during freeze-out or a faster (and thus earlier) release of fission neutrons, which can (partially) prevent this shift and has an impact on the second and rare-earth peak as well.

INTRODUCTION

The astrophysical production site(s) of the *rapid neutron capture process* (r-process) are still unkown. Observations of metal-poor stars reveal that there may be more than one site and that the r-process elements can be divided into two categories: a "weak" component responsible for the production of the lighter elements, and a "strong" component, which produces the heavier elements and shows a remarkable robustness in the abundance pattern [1]. Neutron star mergers (NSM) are a viable candidate for the production of the strong r-process component [2, 3, 4]. In such an extremely neutron-rich environment, the neutron-to-seed ratio can reach 1000 and the reaction path includes several fission cycles, which leads to a robust final abundance distribution. Therefore, the fission treatment becomes an important part of nucleosynthesis calculations in NSMs. As there are not many experimental data that are relevant for fissioning nuclei on the r-process path, there exist many different predictions for the fission barriers and the fragment distributions. We explore different models and show that the choice of (a set of) fission barriers and fission fragment distribution model has a large impact on the final abundance distribution.

CETUP 2015 – Workshop on Dark Matter, Neutrino Physics and Astrophysics and PPC 2015 – IXth International Conference on Interconnections between Particle Physics and Cosmology*
AIP Conf. Proc. 1743, 040004-1–040004-6; doi: 10.1063/1.4953296
Published by AIP Publishing. 978-0-7354-1400-6/$30.00

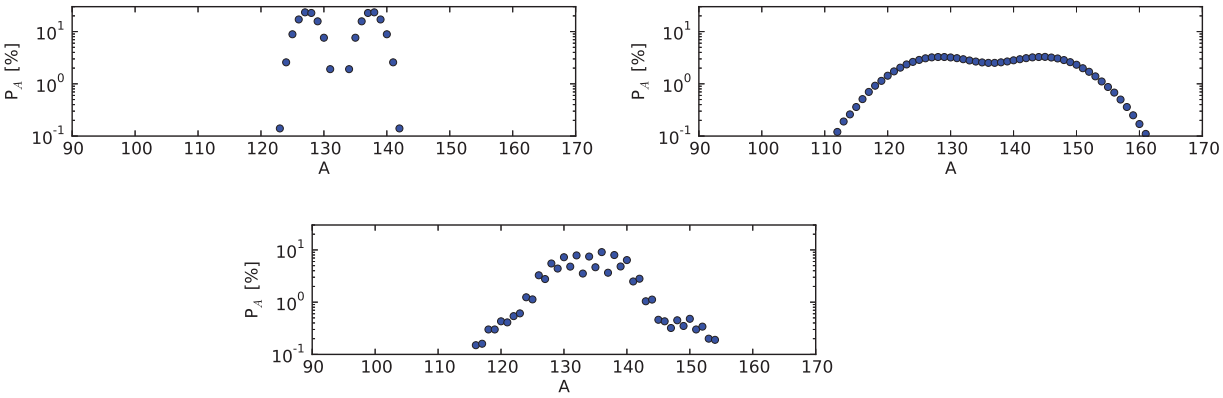

FIGURE 1. Fission fragment distributions for the models considered in our calculations, here for the case of neutron-induced fission of ^{274}Pu (top left: Panov et al. 2008 [9], top right: Kodama & Takahashi 1975 [7], bottom: ABLA07 (Kelic et al. 2008) [10]). For this reaction Panov et al. (2008) predicts 9, ABLA07 7 released fission neutrons. Kodama & Takahashi (1975) and Panov et al. (2001) do not predict any fission neutrons. The distribution for the latter model consists only of two products with $A_1 = 130$ and $A_2 = 144$.

Nuclear mass models and fission fragment distribution models

The r-process operates in the extremely neutron-rich part of the nuclear chart. Therefore, the masses of most nuclei on the reaction path are not (yet) determined experimentally and one has to rely on predictions based on a nuclear mass model. Mass models can differ substantially in their extrapolations towards the neutron drip-line and in their fission barrier predictions [5]. Therefore, the use of different mass models gives rise to different abundance distributions, underlining the large nuclear uncertainties that are still present in r-process nucleosynthesis calculations. Fission fragment distribution models are used to statistically predict the fission fragment yields of each fissioning nucleus. While older models often use simple parametrizations, more sophisticated models are tested on known fission data and take into account shell effects of parent nuclei and fragments. In each fission reaction, there is a possibility of fission neutrons to be emitted. For experimentally studied fission reactions, the number of fission neutrons has been found to be 2 – 4, but it is known to increase with mass number as heavy nuclei become more neutron-rich [6]. If a daughter nucleus is very neutron-rich, additional neutrons can be emitted via photodissociations. In this work we use and compare four different fission fragment distribution models that vary in complexity: (a) Kodama & Takahashi (1975) [7], (b) Panov et al. (2001) [8], (c) Panov et al. (2008) [9], and (d) ABLA07 (Kelic et al. 2008) [10]. The fragment yields predicted by these models on the example of fissioning ^{274}Pu are shown in Figure 1. It can be seen that not only the range of possible fragments differs considerably in each model, but also the predicted amount of fission neutrons.

METHOD

Our nucleosynthesis calculations are based on a NSM simulation with two 1.4 $M_\odot$ neutron stars from Rosswog et al. (2013) [11]. We use 30 representative fluid trajectories, covering all the conditions in the ejected matter and providing the temperature, density and electron fraction within the ejected material up to a time of $t_0 = 13$ ms. To account for the expansion and cooling phase, we extrapolate using the following prescriptions:

$$\rho(t) = \rho_0 \left(\frac{t}{t_0}\right)^{-3} \tag{1}$$

$$T(t) = T[S, \rho(t), Y_e(t)], \tag{2}$$

with time t, density ρ, temperature T, entropy S and Y_e being the electron fraction of the fluid element. The index 0 denotes the values at t_0. The temperature is calculated at each timestep using the equation of state of Timmes & Swesty (2000) [12].

We utilize the extended nuclear network WINNET [13] with more than 6000 isotopes up to Rg. Our sets of reaction rates utilized are based on masses from the *Finite Range Droplet Model* (FRDM; [14]), the *Extended Thomas Fermi Model with Strutinsky Integral* (with shell quenching) (ETFSI-Q; [15, 16]), both in combination with the statistical model calculations of [17] for $Z \leq 83$, and on the *Hartree-Fock-Bogoliubov Model* (HFB-14; [18, 19]), respectively. Theoretical β-decay rates are taken from [20], experimental data from the nuclear database NuDat2 [21]. The neutron capture rates on heavy nuclei ($Z > 83$) as well as the neutron-induced fission rates are from [22], while the β-delayed fission rates are taken from [23]. In our calculations, we refer to the combined application of these basic sets of reaction rates as *original*. We also test the effect of very recent advances in β-decay half-life predictions [24, 25].

RESULTS

Final abundance distributions for each fission fragment distribution model are shown in Fig. 2 for the FRDM mass model. The differences in the models are clearly reflected in the shape of the second r-process peak (mass range $120 < A < 140$) in the final abundances: The two models with the narrowest distribution range (Panov et al. 2001 & 2008) produce a distinct peak, followed by a region of underproduction compared to the solar r-abundances between $140 < A < 170$. The Kodama & Takahashi model, on the other hand, features an extremely broad distribution of fission fragments, which leads to an overproduction of nuclei beyond the second peak. The ABLA07 model shows the best overall agreement with the solar r-abundances. The remaining underproduction of $140 < A < 170$ nuclei is an effect of the mass model and did not appear when we repeated the calculations with the ETFSI-Q and the HFB-14 models in combination with the ABLA07 model.

The Impact of Late Neutron Captures

Figure 2 reveals that the position of the third peak in our final abundance distributions is always shifted towards heavier mass numbers compared to the solar distribution. This phenomenon appears not only for the FRDM mass model, but also when the ETFSI-Q or the HFB-14 mass models are applied. However, we observe that at the time of r-process freeze-out (from (n,γ)-(γ,n) equilibrium), the third peak is still in line with the solar abundance peak, with the shift happening only later. It is caused by late neutron captures by third peak nuclei, the neutrons being continuously supplied by the fissioning of material above $A \simeq 240$. Furthermore, mainly nuclei beyond the second peak are affected, since (a) the neutron capture cross sections depend on the mass number of the capturing nuclei and are generally larger for higher mass numbers, and (b) the abundance pattern of the second peak is dominated by the fission fragment production, even after the r-process freeze-out.

To further illustrate the importance of fission neutrons after the freeze-out, we have run several calculations with both FRDM and HFB-14 where we have switched off certain types of reactions after the freeze-out. (1) The dashed

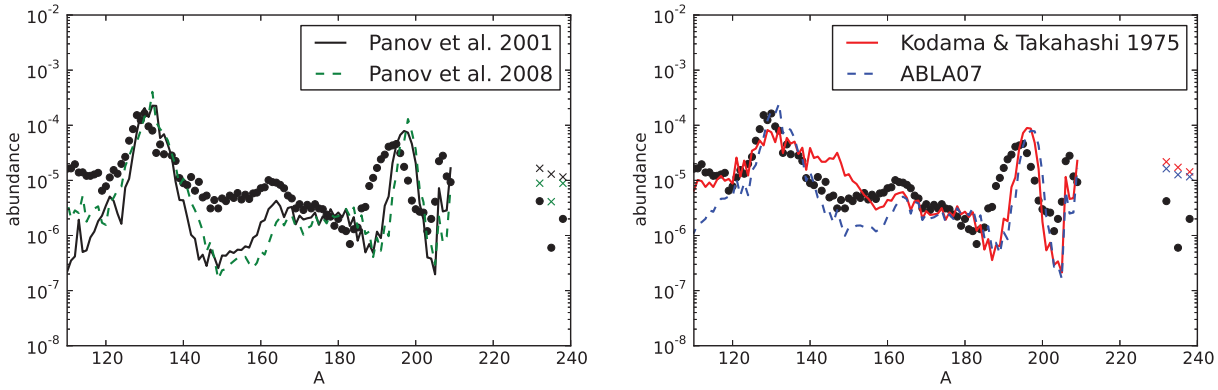

FIGURE 2. Final abundances of the integrated ejecta around the second and third peak for a NSM [11] at a simulation time $t = 10^6$ s, employing the FRDM mass model combined with four different fission fragment distribution models (see text). For reasons of clarity the results are presented in two graphs. The abundances for Th and U are indicated by crosses. The dots represent the solar r-process abundance pattern [26].

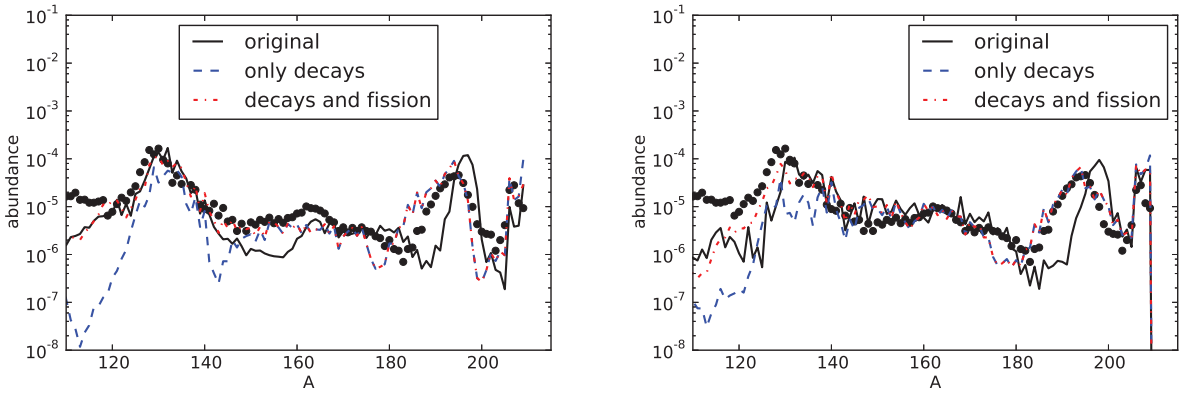

FIGURE 3. Final abundance distribution for cases where only certain types of reactions are allowed to proceed after freeze-out (dashed line: only decays except for fission; dot-and-dashed line: decays including fission) for FRDM (left) and HFB-14 (right). The solid line represents the original calculation where neutron captures are also allowed after freeze-out. All cases use ABLA07.

lines in Fig. 3 (labelled "only decays") represent the cases where only decay reactions are allowed after the (n,γ)-(γ,n) freeze-out (without fission). In this artificially created scenario the only possibility for nuclei after the freeze-out is to decay to stability, without the option to fission or capture neutrons. In fact, a small shift of the third peak to lower mass numbers can be observed during this phase, as β-delayed neutrons cause the average mass number to decrease. In addition, since fission is not allowed either, the second peak consists of just the material that was present there at freeze-out, but the composition is (slightly) modified due to the combined effects of β-decays and β-delayed neutrons. (2) If we also allow for fission in addition to the decay reactions (dot-and-dashed lines in Fig. 3), the second peak is nicely reproduced by fission fragments for both mass models and the third peak is still not affected. (3) However, a notable difference between the two mass models can be seen for the final abundance distribution including also final neutron captures (denoted as "original" in Fig. 3), indicating that for HFB not only the position of the third peak is influenced by late neutron captures, but also the position of the second peak. On the other hand, the behaviour is reversed for the mass region $140 < A < 160$, where large deviations can be observed compared to the original calculation for FRDM, since in the original case neutron captures move material up to higher masses, creating the underproduction we have discussed before. This indicates that when also neutron captures and all other reactions are permitted after freeze-out (i.e., the original calculation), major changes in the abundance pattern can still occur. The third peak moves to higher masses for all mass models discussed here.

Neutron captures after the freeze-out are responsible for the shift in the third peak, with a large amount of fission neutrons being released in fission reactions happening around or after the freeze-out. If those neutrons were released earlier, they would be recycled into the r-process at a time when (n,γ)-(γ,n) equilibrium prevails. In this context, the role of beta-decays (especially of the heaviest nuclei) is essential, as they determine the speed at which heavy (fissioning) nuclei are produced, as well as the time duration for which fissioning nuclei still exist.

In order to test the potential impact of β-decays on the position of the third peak and the final abundance pattern in general, we employ two newly calculated sets of half-lives from Marketin et al. (2015, in preparation) [24] and Panov et al. (2015) [25]. Both new sets predict shorter half-lives for the majority of neutron-rich nuclei in the nuclear chart compared to the previously used half-lives [20]. However, there are some decisive differences. In Figure 4 we present a comparison of the new β-decay rates with the rates that we have used before. The Panov et al. (2015) set does not predict significantly faster rates far from stability, but in fact even noticeably slower rates (shown in blue) around $N = 162$ close to the neutron drip line. The faster rates (red) closer to stability only come into effect after freeze-out. The Marketin et al. (2015) calculations, on the other hand, predict faster rates for all nuclei on the r-process path beyond $N = 126$. The impact on the final abundances can be seen in Figure 5, where we present calculations performed using the Marketin et al. (2015) rates as well as the Panov et al. (2015) rates together with the FRDM model. Note that the former have been calculated using a different mass model, so they are not fully consistent with FRDM. The Panov et al. (2015) rates are based on FRDM.

The Marketin et al. (2015) half-lives show a strong effect on the final abundances, broadening the low-mass flank of the third peak and increasing the abundances around the rare-earth peak. In fact, the broadening of the peak to lower

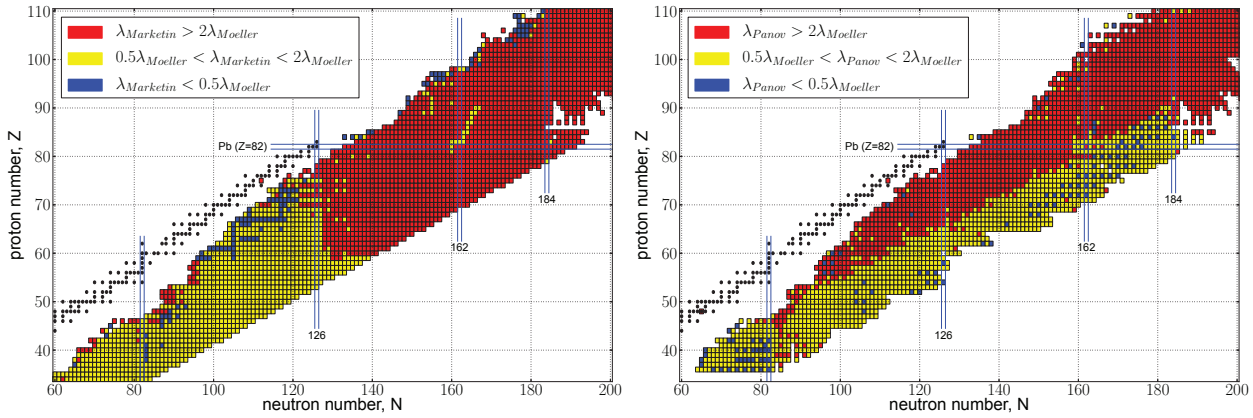

FIGURE 4. Left: Comparison of the new Marketin et al. (2015) β-decay rates with the old Möller et al. (2003) rates. A red square means that the Marketin et al. (2015) β-decay rate ($\lambda_{Marketin}$) of the corresponding nucleus is more than two times faster than the Möller et al. (2003) rate, while a blue square signifies that it is slower by more than a factor of 2. If the two rates are within a factor of 2 to each other, the square is coloured yellow. Right: Same for the new Panov et al. (2015) rates.

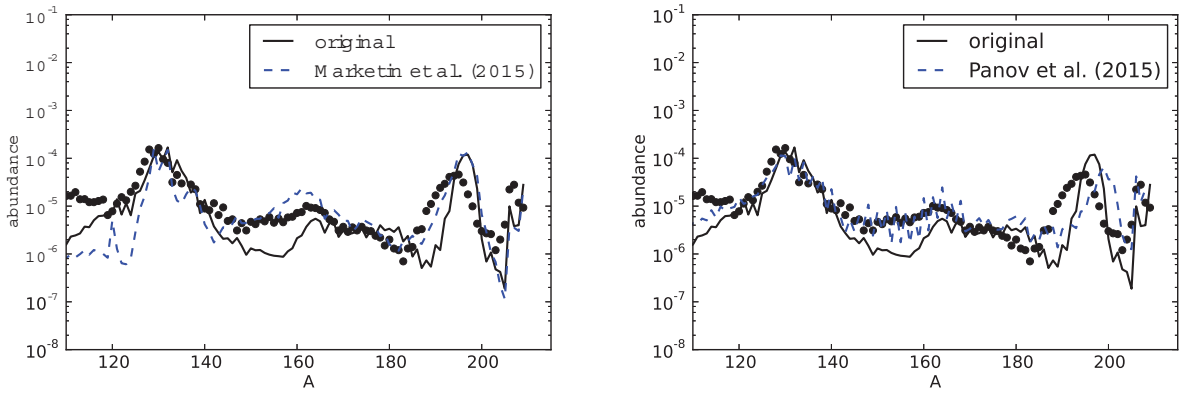

FIGURE 5. Left: Final abundance distribution for a calculation using the Marketin et al. (2015) rates together with the FRDM mass model and ABLA07. As a reference the FRDM, ABLA07 calculation from Fig. 2 is included. Right: Same, but with the Panov et al. (2015) rates.

mass numbers strongly improves the shape of the peak and even a slight shift of the position to lower masses can be observed. The Panov et al. (2015) rates have a different effect. Here the β-decays are faster for nuclei with $N = 126$ along the r-process path (before the freeze-out). Therefore the reaction flux proceeds faster in this region before it is held up afterwards at higher mass numbers, which means that less matter is accumulated in the peak. As a result, the height and shape of the third peak matches the solar peak very well. However, as the abundances of the nuclei in the peak are lower by roughly a factor of 2, each nucleus in the third peak can capture double the amount of neutrons and the effect of the third peak shift is increased. Furthermore, these rates show strong odd-even dependencies in the mass region $140 < A < 170$, a quality which is reflected in the final abundances in this mass region.

CONCLUSIONS

We have shown that the r-process yields in neutron star merger (NSM) ejecta are strongly affected by the adopted model for fission fragment distributions. Among the models utilized here, we find that the best agreement with the r-process pattern of solar abundances is achieved with the ABLA07 model, which was tested not only for experimental fission fragment distrubutions, but also for the fragment distributions from extended heavy ion collision yields and thus goes far beyond earlier pure extrapolations of experimental fission fragment data. Similar studies with different fission fragment distribution models have been performed recently [27].

In neutron-rich NSM nucleosynthesis, the third peak in the final abundance distribution shifts towards higher masses if after the r-process freeze-out the conditions for further neutron capture reactions prevail. The two main factors that affect these conditions are temperature and neutron density. If the neutron density is high enough, several neutron captures after freeze-out shift the peak. In this context, we have explored the effect of new theoretical β-decay predictions [24, 25] on the shape and the position of the third peak. In this case the reaction flux is accelerated, leading to an earlier release of the fission (and β-delayed) neutrons, where some of them are recycled in the (n,γ)-(γ,n) equilibrium that is present before the freeze-out, improving the final abundance pattern compared to the solar abundances.

REFERENCES

[1] C. Sneden, J. E. Lawler, J. J. Cowan, I. I. Ivans, & E. A. Den Hartog, ApJS 182, 80 (2009).
[2] C. Freiburghaus, S. Rosswog, & F.-K. Thielemann, ApJ 525, L121 (1999).
[3] A. Bauswein, S. Goriely, & H.-T. Janka, ApJ 773, 78 (2013).
[4] S. Rosswog, O. Korobkin, A. Arcones, F.-K. Thielemann, & T. Piran, MNRAS 439, 744 (2014).
[5] I. Petermann, K. Langanke, G. Martinez-Pinedo, et al., European Physical Journal A 48, 122 (2012).
[6] E. P. Steinberg & B. D. Wilkins, ApJ 223, 1000 (1978).
[7] T. Kodama & K. Takahashi, NuPhA 239, 489 (1975).
[8] I. V. Panov, C. Freiburghaus, & F.-K. Thielemann, Nuclear Physics A 688, 587 (2001).
[9] I. V. Panov, I. Y. Korneev, & F.-K. Thielemann, Astronomy Letters 34, 189 (2008).
[10] A. Kelic, M. V. Ricciardi, & K.-H. Schmidt, in *Dynamical Aspects of Nuclear Fission 6*, Conference Proceedings (World Scientific, 2008), p. 203.
[11] S. Rosswog, T. Piran, & E. Nakar, MNRAS 430, 2585 (2013).
[12] F. X. Timmes & F. D. Swesty, ApJS 126, 501 (2000).
[13] C. Winteler, R. Käppeli, A. Perego, et al., ApJL 750, L22 (2012).
[14] P. Möller, J. R. Nix, W. D. Myers, & W. J. Swiatecki, Atomic Data and Nuclear Data Tables 59, 185 (1995).
[15] Y. Aboussir, J. M. Pearson, A. K. Dutta, & F. Tondeur, Atomic Data and Nuclear Data Tables 61, 127 (1995).
[16] J. M. Pearson, R. C. Nayak, & S. Goriely, Physics Letters B 387, 455 (1996).
[17] T. Rauscher & F.-K. Thielemann, Atomic Data and Nuclear Data Tables 75, 1 (2000).
[18] S. Goriely, S. Hilaire, & A. J. Koning, A&A 487, 767 (2008).
[19] S. Goriely, S. Hilaire, A. J. Koning, M. Sin, & R. Capote, Phys. Rev. C 79, 024612 (2009).
[20] P. Möller, B. Pfeiffer, & K.-L. Kratz, Phys. Rev. C 67, 055802 (2003).
[21] NuDat2. 2009, National Nuclear Data Center, information extracted from the NuDat 2 database, URL http://www.nndc.bnl.gov/nudat2/
[22] I. V. Panov, I. Y. Korneev, T. Rauscher, et al., A&A 513, A61 (2010).
[23] I. V. Panov, E. Kolbe, B. Pfeiffer, et al., Nuclear Physics A 747, 633 (2005).
[24] T. Marketin, L. Huther, & G. Martinez-Pinedo, in preparation (2015).
[25] I. V. Panov, Y. S. Lutostansky, & F.-K. Thielemann, Bull. Russ. Acad. Sci. Phys., in press (2015).
[26] C. Sneden, J. J. Cowan, & R. Gallino, Ann.Rev.Astron.Astrophys. 46, 241 (2008).
[27] S. Goriely, J.-L. Sida, J.-F. Lemaitre, et al., Physical Review Letters 111, 242502 (2013).